



# MODELING THE DAMAGE OF WELDED STEEL, USING THE GTN MODEL

El-Ahmar Kadi<sup>1\*</sup>, Benguediab Mohamed<sup>1</sup>, Bouchouicha Benattou<sup>1</sup>, Mazari Mohamed<sup>1</sup>, Zemri Mokhtar<sup>1</sup>

<sup>1</sup>Laboratory of Materials and Reactif Systems, Department of Mechanic, Faculty of Technology, University of Djillali Liabes, BP 89 Ben M'hidi City, Sidi Bel Abbès, 22000, Algeria

\*corresponding author: tel: +213554808798, e-mail: el-ahmar.kadi@gmail.com

## Resume

The aim of our work is the modeling of the damage in the weld metal according to the finite element method and the concepts of fracture mechanics based on local approaches using the code ABAQUS calculates. The use of the Gurson-Tvergaard-Needleman model axisymmetric specimens AE type to three different zones (Base metal, molten metal and heat affected Zone) with four levels of triaxiality (AE2, AE4, AE10 and AE80), we have used to model the behavior of damage to welded steel, which is described as being due to the growth and coalescence of cavities with high rates of triaxiality.

## Article info

### Article history:

Received 10 December 2013

Accepted 12 August 2014

Online 30 November 2014

### Keywords:

Growth of cavities;  
Volume deformation;  
Damage;  
GTN;  
Weld;  
Steel.

Available online: <http://fstroj.uniza.sk/journal-mi/PDF/2014/20-2014.pdf>

ISSN 1335-0803 (print version)

ISSN 1338-6174 (online version)

## 1. Introduction

Simulation of ductile damage behavior of metallic materials known to the development of several continuous models generally observed a large deformations in the past three decades, the evolution of damage in the stress triaxiality is the key to each these studies. Today ductile fracture is governed by three physical mechanisms: initially inexistent nucleation cavities, growth of these cavities in an appropriate loading and finally the coalescence of adjacent cavities. The study of this failure mechanism involves the use of local approaches that are based on knowledge of the field of stress and strain.

McClintock's work and those of Rice and Tracey, based on the growth of cavities, is an undeniable contribution to the development of fracture mechanics. These approaches considered that the rate of growth of the cavities is modeled by an exponential function based on

the rate triaxiality constraints  $\tau$ , defined by the ratio  $\sigma_m/\sigma_{eq}$ . From this work, several models have been proposed, in particular based on continuous damage models (coupled models) as the model of Gurson.

Gurson has developed a constitutive model for porous ductile media based on a rigid-plastic material behaviour and the upper bound theorem of plasticity. Based on detailed phenomenological studies of the behaviour of materials containing periodic distributions of cylindrical and spherical voids.

Our goal is to provide a methodology possibly including finite element modeling to describe the various pathways for study options and choose the most appropriate approach to the description of failure mechanisms of welded steel. We will perform a mechanical characterization to identify the major physical phenomena to be considered in modeling. On this basis, we propose the approach of

a constitutive and a damage criterion specific to welded steel.

## 2. Presentation of the Model GTN

The experimental results indicate the central role of the growth of cavities in ductile metals [1, 2, 3]. All these studies have focused on metallic materials and showed that the cavities formed on the second phase particles, or by decohesion between a particle and the matrix, or the rupture of a particle. The final rupture occurs after the growth phase of adjacent cavities until their final coalescence. Analyzes growth of cavities in infinite plastic material shows that this growth is highly dependent on the hydrostatic stress [4, 5]. And the coalescence of the cavities is generated by a high rate of triaxiality. This prediction was confirmed by a series of specimens tested on more severely notched least in the case of steel [6, 7].

Given the experimental results, there has been a growing interest in the use of the growth and coalescence of cavities to describe ductile metals. Many examples of research focused on the growth of a single cavity in an infinite elasto-plastic solid, for different stress states [4, 8, 9]. Based on analyzes equivalent to a spherical cavity, Gurson developed a model to describe the behavior of a ductile porous solid [10, 11]. In this model the parameter  $f$ , volume fraction of porosity, is the only parameter of material damage and the response is very sensitive to its evolution. This model was extended by Needleman and Rice to account for the germination of cavities [12], and then by Tvergaard and Needleman to reflect the coalescence of cavities [13, 14]. GTN model is based on the micromechanical model developed by Gurson [15]. It allows describing the growth of a spherical cavity in a rigid perfectly plastic matrix leading to the expression of the plasticity criterion given by (1):

$$\Phi = \frac{\sigma_{eq}^2}{\sigma_y^2} + 2 f^* \cdot q_1 \cdot \cosh\left(\frac{3}{2} q_2 \frac{\sigma_m}{\sigma_y}\right) - (1 + q_3 (f^*)^2) = 0 \quad (1)$$

With the constitutive parameters  $q_1$ ,  $q_2$ ,  $q_3$  ( $q_3 = (q_1)^2$ ).

$f^*$  represents the modified volumetric void fraction which is the function of  $f$  defined by:

$$f^* = \begin{cases} f & \text{for } f \leq f_c \\ f_c + \delta(f - f_c) & \text{for } f > f_c \end{cases}$$

with

$$\delta = \frac{f_u^* - f_c}{f_F - f_c} \quad (2)$$

Where  $f_u^*$  is the ultimate value of  $f^* = 1/q_1$ ,  $f_F$  the volume fraction of void in the final rupture and  $f_c$  the critical volume fraction of void.

The volume fraction of void  $f$  is divided into a new term nucleation cavities  $f_{\text{nucleation}}$  and The change of the volume fraction of cavities is given by the following expression:

$$df = df_{\text{nucleation}} + df_{\text{growth}}$$

with

$$df_{\text{growth}} = (1 - f) d\varepsilon_{kk}^p \quad (3)$$

and

$$df_{\text{nucléation}} = a d\varepsilon_{eq}^p \quad (4)$$

where  $\varepsilon_{kk}^p$  the total of normal component of the plastic deformation,  $\varepsilon_{eq}^p$  the equivalent plastic strain. The parameter of germination «a», which is selected in the event that the void nucleation follows a normal distribution, depends on the equivalent plastic strain.

To calculate a cracked structure using the GTN model, several parameters are required:

- Generally, the constitutive parameters are fixed at  $q_1 = 1.5$ ,  $q_2 = 1$  et  $q_3 = (q_1)^2$ . In a recent study, Perrin and Leblond [16] have demonstrated the existence of a correlation between the parameter  $q_1$  and porosity  $f$  and for a porosity tends to zero  $q_1$  takes the value about 1.47. Under a wide bibliographic study on the model parameters of GTN, it was shown that the parameter  $q_1$  takes values between 1.1 and 1.5 [17].

- $f_0$ , initial porosity is a parameter related to the material (measured from microscopic observations or estimated from the formula of Franklin).

- $\delta$  which represents the slope acceleration of the growth of porosity and «a» parameter of the continuous germination, may be arbitrarily set or adjustable parameters considered.

- $f_c$ , which corresponds to the onset of coalescence, is an adjustable parameter using numerical simulation.

### 3. Law of Behavior

To determine the behavior law of welded steel, was used an experimental test geometry corresponds to ASTM D638 M1A, Fig. 1. The test was made on Instron tensile machine, the mechanical properties of welded steel for

a speed of  $0.001 \text{ s}^{-1}$  and at room temperature  $23^\circ \text{ C}$  are given as follows:

BM ( Base Metal ) :

$$E = 183 \text{ GPa and } \sigma_e = 300 \text{ MPa and } \nu = 0.3 .$$

WM ( Weld Metal ) :

$$E = 180 \text{ GPa and } \sigma_e = 400 \text{ MPa and } \nu = 0.3 .$$

HAZ ( Heat Affected Zone ) :

$$E = 450 \text{ GPa and } \sigma_e = 205 \text{ MPa and } \nu = 0.3 .$$

Working on axisymmetric notched specimens (AE), it is possible to study the multiaxial stresses, only using a tensile test. These samples are used to study conditions of plane strain and plane stress.

For a notched specimen, as the elastic limit is not exceeded the maximum stress is in the bottom of the notch by the phenomenon of stress concentration. The elastic limit is reached first at this point. If the test continues to be deformed plastically, deformed zone extends and eventually invade the entire notched section. The load then reaches the limit load of the specimen; it is greater than it would be without fault (notched). Consider for that first a cylinder of material in the notch portion of the specimen, if it were isolated, lengthen it along its axis and along its diameter would shrink in order to maintain a constant volume. Included in the notch between the two parties unnotched remaining elastic and deform slightly, it can only contract in the same way and it appears radial stress of tension. To satisfy the yield criterion (von Mises or Tresca), it is necessary to increase all the axial stress. Thus, the plastic deformation confined raises the general level of stress and stress triaxiality rate  $\beta$ . This is defined by the equation (5):

$$\beta = \frac{\sigma_m}{\sigma_{eq}} \quad (5)$$

$\sigma_m$  : Mean stress defined as

$$\sigma_m = \left( \frac{1}{3} (\sigma_{11} + \sigma_{22} + \sigma_{33}) \right) \quad (6)$$

$\sigma_{eq}$ : Von Mises equivalent stress.

For a cylindrical specimen having a groove notch root radius ( $R$ ) leaving a collar radius ( $a$ ) in the minimum section, the calculation of stress distributions and deformations is complicated and cannot be completely solved analytically. Simplifying assumptions are necessary such as equality between radial and tangential distortions in the minimum section when  $Z = 0$ . It follows that the radial and tangential stresses are equal and that deflector is independent of the radial coordinate ( $r$ ) in this section. With these assumptions, the equations of equilibrium and the plasticity criterion, it is shown that:

$$\frac{d\sigma_{rr}}{d_r} = -\frac{\sigma_{eq}}{\rho} \quad (7)$$

With ( $r$ ) the radius of curvature of the lines isostatic, where they intercept the plane  $Z = 0$ . Bridgman [18] assumed that the isostatic lines can be treated as circles that intersect at right angles the surface of the ring is cut. [19] The radius of curvature ( $\rho$ ) is given by the relation (7).

The integration of the differential equation (6) leads to (8):

$$\rho = \frac{a^2 + 2aR - r^2}{2r} \quad (8)$$

The average axial stress  $\bar{\sigma}_{zz}$  that is to say the load on the specimen is given by the expression (9):

$$\text{And } \left\{ \begin{array}{l} \sigma_{rr} = \sigma_{\theta\theta} = \sigma_{eq} \ln\left(1 + \frac{a^2 - r^2}{2aR}\right) \\ \sigma_{zz} = \sigma_{eq} \left[1 + \ln\left(1 + \frac{a^2 - r^2}{2aR}\right)\right] \end{array} \right. \quad (9)$$

$$\bar{\sigma}_{zz} = \sigma_{eq} \left(1 + \frac{2R}{a}\right) \ln\left(1 + \frac{a}{2R}\right) \quad (10)$$

The rate of stress triaxiality is maximum on the axis of the specimen such that:

$$\frac{\sigma_m}{\sigma_{eq}} = \frac{1}{3} + \ln\left(1 + \frac{a}{2R}\right) \quad (11)$$

#### 4. Choice of Geometry

We chose to work with AE notched axisymmetric specimens at four different radii of curvature in order to study the influence of the rate of stress triaxiality on the behavior of the material "damage". The four radii studied are:  $R = 80$  mm (AE80), 10 mm (AE10), 4 mm (AE4) and 2 mm (AE2). For each radius we make the same test for three different zones (BM, WM & HAZ) to see the influence of stress triaxiality. We consider the simplest analysis traction monotonous. Given the imperfections of the model, we clear despite all the benefits of its components dependent plasticity criterion. Tensile tests on the specimens were carried out in AE imposed displacement. Geometry axisymmetric notched specimens (AE) Hourglass type (Fig. 2) such that the total length is 46 mm, the width of the shaft is 10 mm, and the notch root is 5 mm. The height of the scored area will vary with the radius of curvature ( $R = 80, 10, 4, 2$  mm).

#### 5. Mesh

Notched geometries were studied by symmetry (axisymmetric), only half of the specimen is meshed with axisymmetric element quadratic reduced integration (called cax4r). Thus, by symmetry, it is possible to mesh the half-length to represent the entire structure. In the notched zone, the mesh is finite, contrary to the smooth zone where it is coarser.

This copy of the article was downloaded from <http://www.mateng.sk>, online version of Materials Engineering - Materiálové inžinierstvo (MEMI) journal, ISSN 1335-0803 (print version), ISSN 1338-6174 (online version). Online version of the journal is supported by [www.websupport.sk](http://www.websupport.sk).

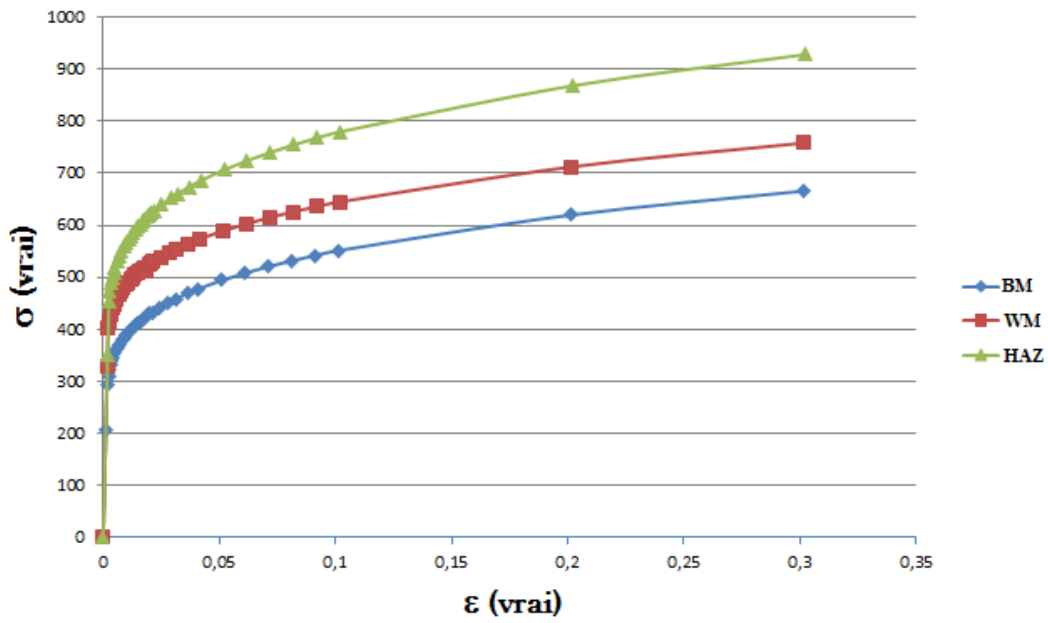


Fig. 1. A48 Steel curve (BM, WB and HAZ).  
(full colour version available online)

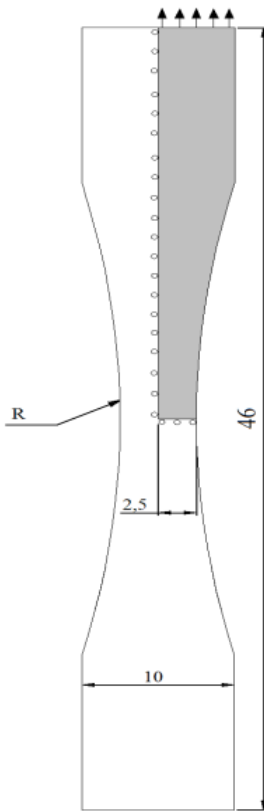


Fig. 2. Notched specimen type hourglass with a radius of curvature  $R$  (mm).

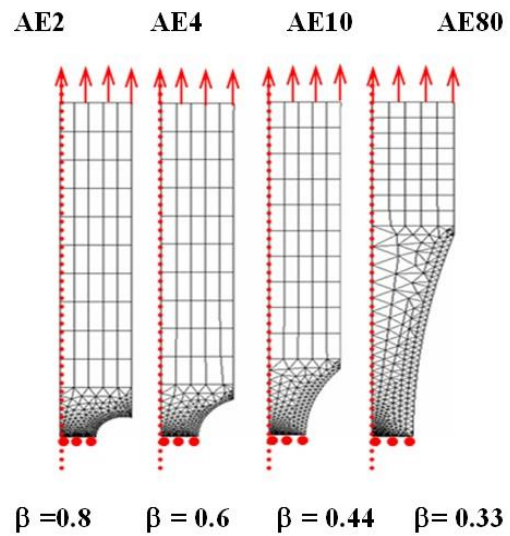


Fig. 3. Mesh specimens AE.  
(full colour version available online)

The total number of node varies depending on the geometry studied: 905 nodes and 280 elements for the AE80, 1080 nodes and 345 elements for the AE10, 1273 nodes and 400 elements for AE4, 1527 nodes and 400 elements for the AE2 . Fig. 3 shows the mesh sizes used in the region of the notch and the entire half-length.

## 6. Results and Discussion

The finite element method has allowed us to numerically analyze and determine the distribution of strain fields adjacent of the notch. These results are obtained from analysis tests on four specimens tensile triaxiality different  $\beta = 0.33, 0.44, 0.6$  and  $0.8$ , and from three different zone (BM, WM & HAZ).

Fig. 4 presents the evolution and the longitudinal strain localization in useful zones. We note firstly that the deformations are concentrated in bottom of notch, the concentration decreases as one moves away from it, secondly this concentration increases with increasing radius curvature, same things for different zone.

Fig. 5 shows the variation of the equivalent stress of Von Mises function of time produced by the finite element and measured in the center of the specimen (the most solicited) for the same tensile tests of analysis with the four different triaxiality  $\beta = 0.33, 0.44, 0.6$  and  $0.8$  in different zone of weld. The results show that the equivalent stress changes when the triaxiality increases (Fig. 5).

Fig. 6 (a, b, c and d) shows the variation of stress and strain in the center of the specimen as a function of time in order to study the sensitivity and the effect of triaxiality. Observed when the triaxiality increases, the maximum stress increases but the deformation remains the same. For low

triaxiality maximum stress is almost the same.

Fig. 7 shows the true stress and the change in volume as a function of axial true strain, if we compare the results of true stress as a function of axial true strain for different triaxiality, we can see that all segments OA, AB, BC, CD and DE have the same shape, which explains that OA is the linear part of the curve. It corresponds to the reversible deformation. AB: There is loss of linearity between load and deformation; usually B is considered the limit of plasticity, therefore plastic deformation beyond this limit.

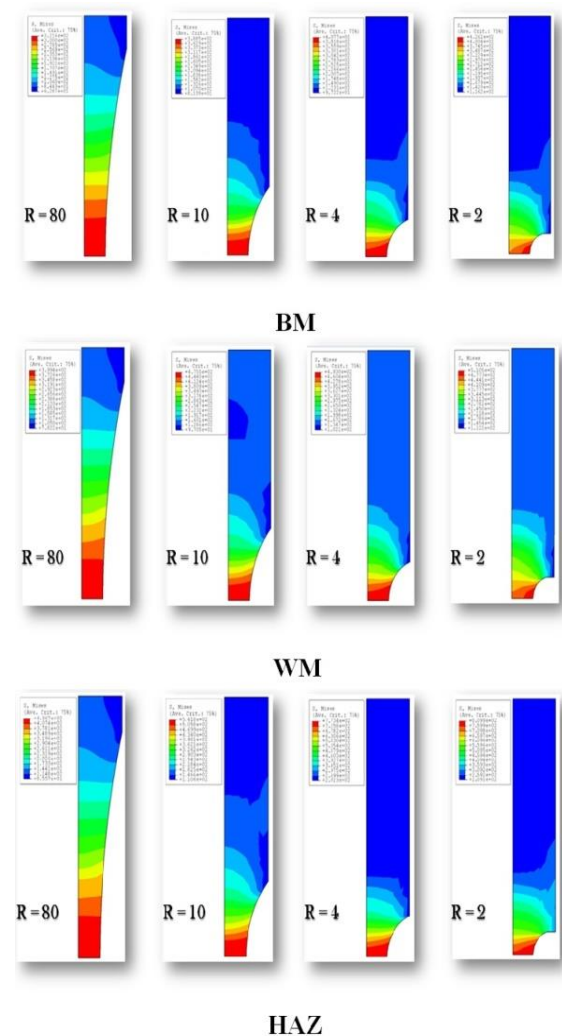


Fig. 4. Strain Fields.  
(full colour version available online)

This copy of the article was downloaded from <http://www.mateng.sk>, online version of Materials Engineering - Materiálové inžinierstvo (MEMI) journal, ISSN 1335-0803 (print version), ISSN 1338-6174 (online version). Online version of the journal is supported by [www.websupport.sk](http://www.websupport.sk).

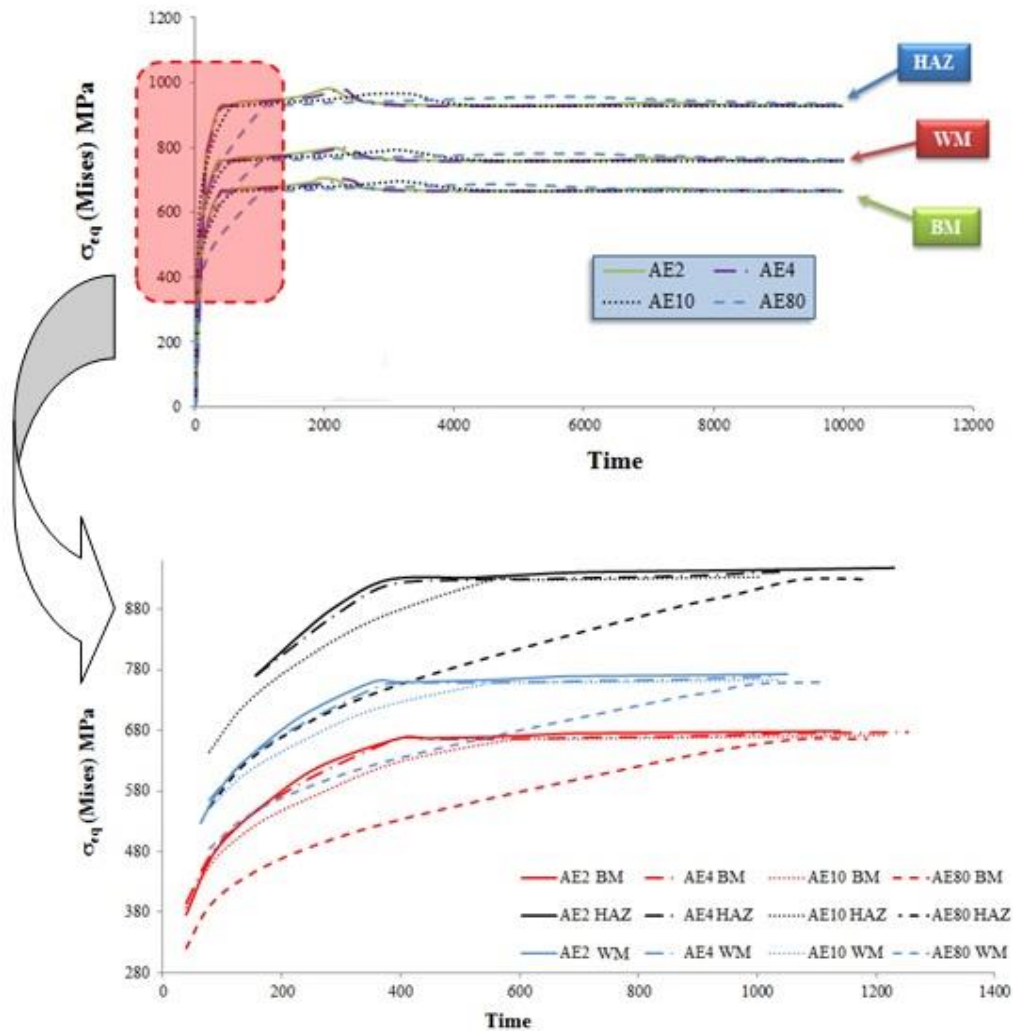


Fig. 5. Evolution of the equivalent stress versus time. (full colour version available online)

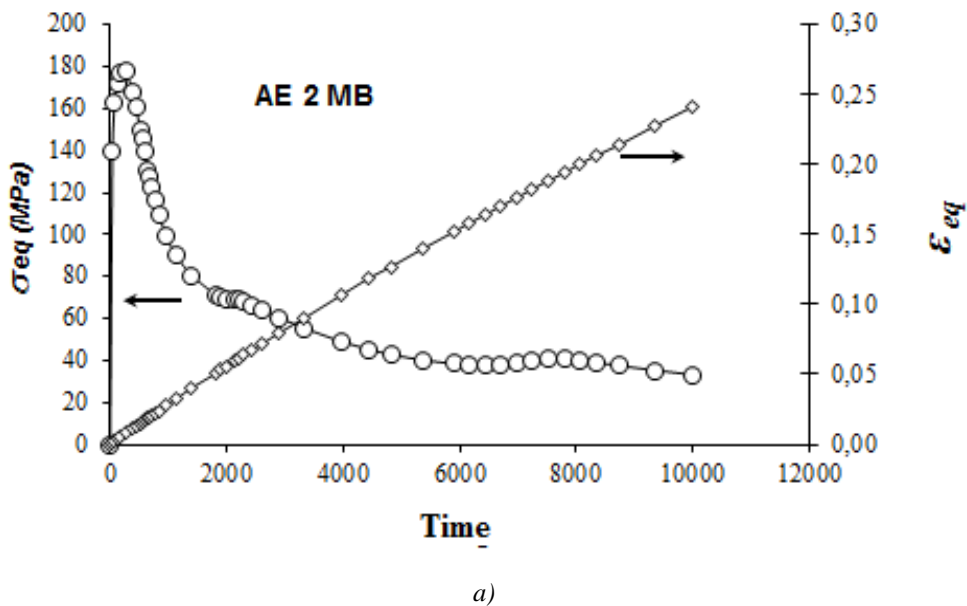
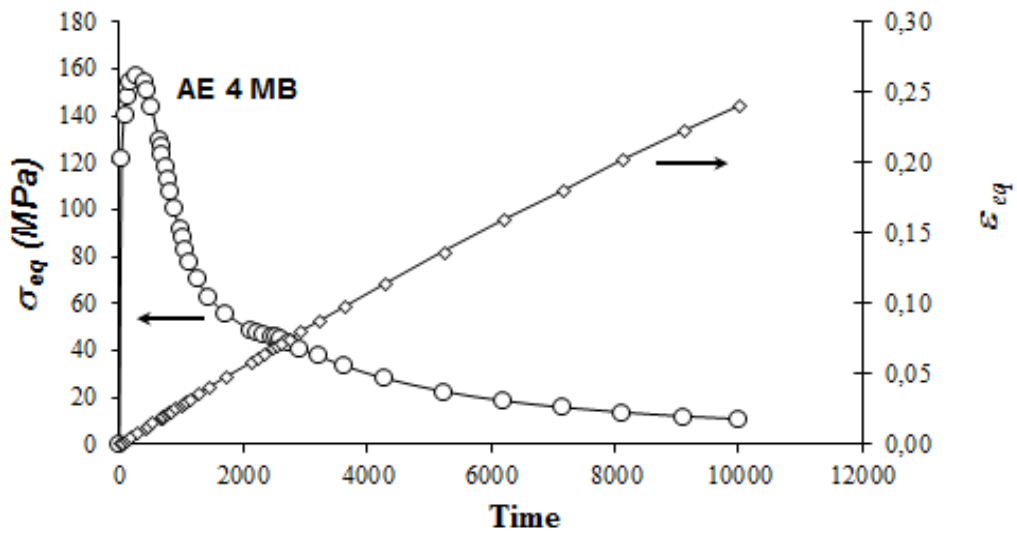
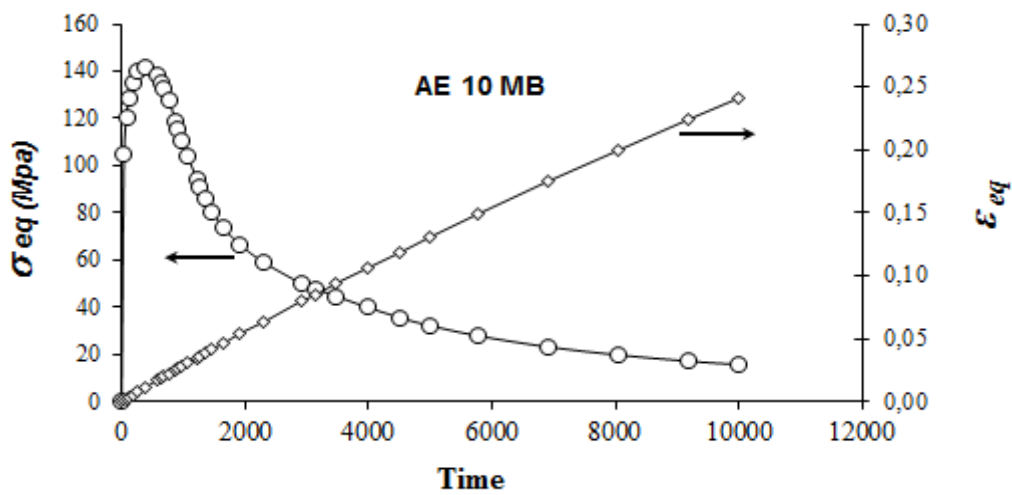


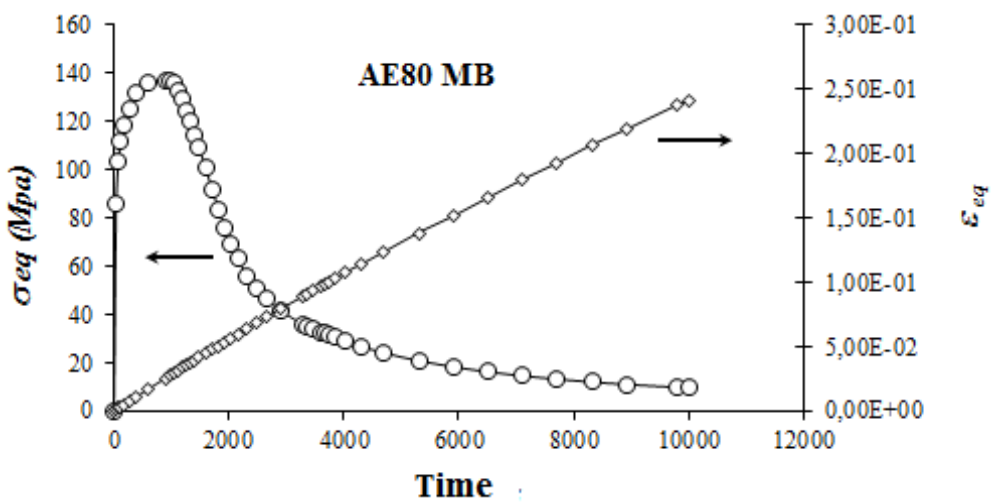
Fig. 6. Evolution of the stress - strain versus time.



b)



c)



d)

Continuing of Fig. 6. Evolution of the stress - strain versus time.



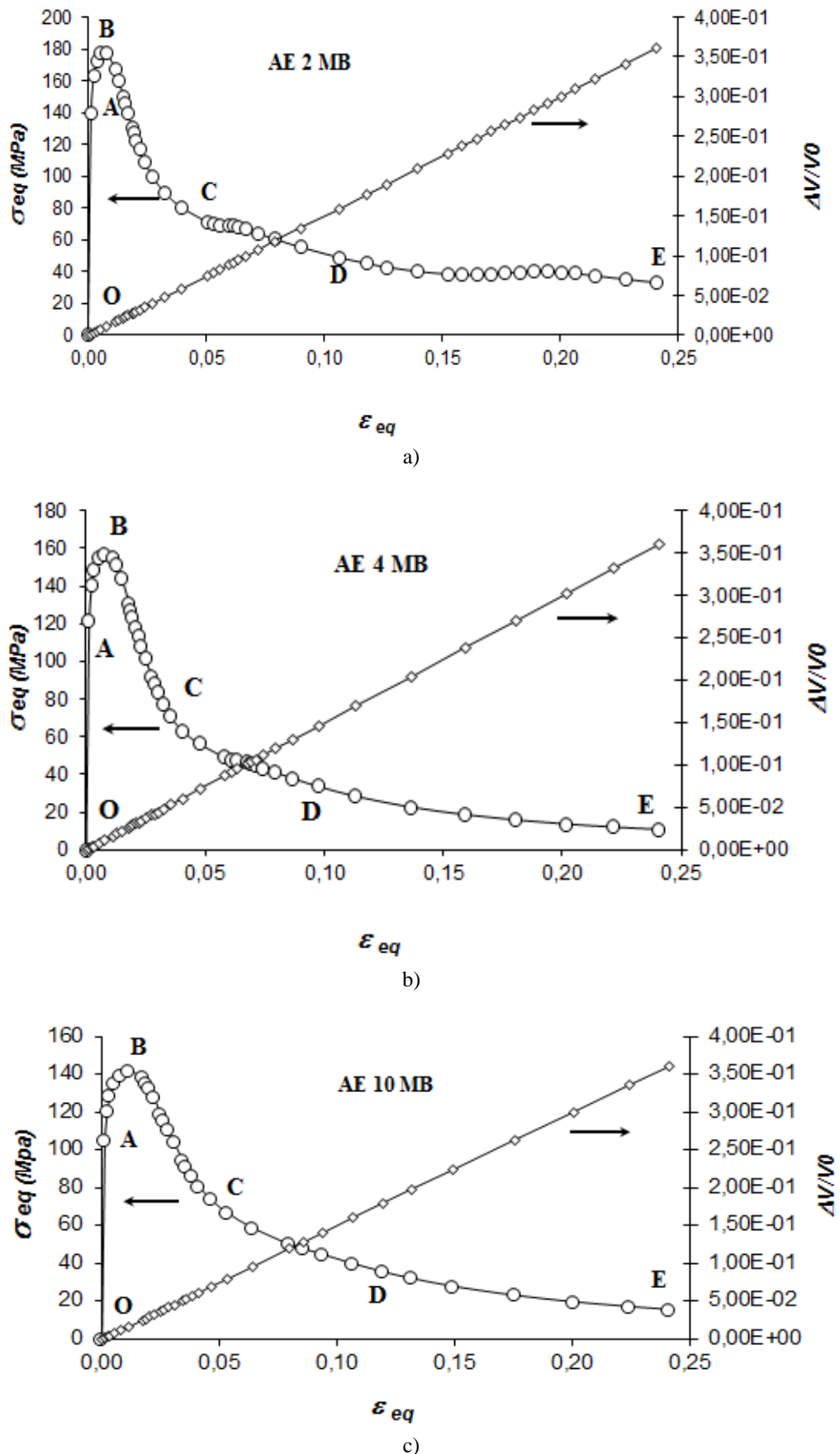
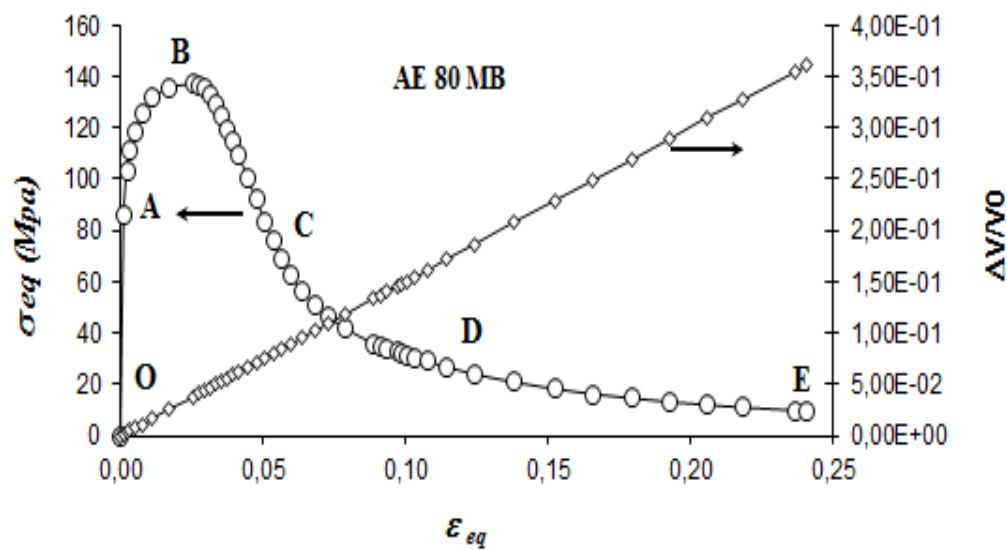


Fig. 7. The variation of the true stress and volume depending on the axial deformation (true).



d)

Continuing of Fig. 7. The variation of the true stress and volume depending on the axial deformation (true).

BC striction zone, the point B is associated with the beginning of the formation of a striction, which may notice a decrease in the load. The CE segment, we can say that this is the area that necking starts the CD section: a large-scale reorganization of the molecular structure of the sample. That changes shape all depends on the triaxiality given our specimens. DE is the same part of the four curves, which allows us to observe the propagation of necking which is a more or less constant load.

## 7. Conclusions

The Gurson-Tvergaard-Needleman model usually used for metallic materials has been used here to model the behavior of damage welded steel. The damage in this model is described as being due to the growth of cavities, represented by parameters.

The model helped to account for all the mechanical results and determine an approach related to failure mode and fracture crazing, a criterion coalescence of cavities with rate triaxiality criterion and coalescence of cavities in the high rate of triaxiality. The maximum principal stress has been determined as the criterion for ductile-brittle transition explaining the failure modes in

tension. The damage is taken into account by adjusting the parameters of the model on the evolution of volumetric strain, as well as the traction hook translating the softening of charge due to the strong growth of cavities.

The relative error is with direction of least squares. The method of identification that we have just used is unfortunately not optimal, and the variation of a parameter is likely to involve.

In modeling, we were interested in the variation and optimization of the parameters to describe the behavior of welded steel class. The digital shutter consisting then with the exploration of the parameters employed in our computer code. Thanks to the simplicity of the model, test them analyses gave promising results in different case. The whole of our tests of analysis in terms of local curves are acceptable even in the case of strong maps. Thus, the model predicts the evolution of the stress - strain in the calculation.

## References

- [1] D. E. Puttick: Philosophical magazine 4 (1959) 964-969.
- [2] H. C. Rogers: Transactions AIME 218 (1960) 498-506.



- [3] L .M. Brown, J. D. Embury: In: Proc. 3rd International conference on strength of metals and alloys, Inst. of metals Cambridge 1973, pp. 164-169.
- [4] J. R. Rice, D. M. Tracey: Journal of the Mechanics and Physics of Solids. Phys. Solids, 17 (1969) 201-217.
- [5] F. A. McClintock: J. Appl. Mechanics 35 (1968) 363-375.
- [6] J. W. Hancock, A. C. Mackenzie: J. Mechanics and Physics of Solids 24 (1976) 147-160.
- [7] J. W. Hancock, D. K. Brown: J. Mechanics and Physics of Solids 31 (1983) 1-24.
- [8] F. A. McClintock: J. Applied Mechanics 35 (1968) 363-375.
- [9] B. Budiansky, J. W. Hutchinson, S. Slutsky: In: Void growth and collapse in viscous solids, in : Mechanics of solids, Ed. H.G. Hopkins and M.J. Sewell, The Rodney Hill 60th anniversary volume, Pergamon 1982, pp. 13-45.
- [10] A. L. Gurson: J. Eng. Mater. and technol. 99 (1977) 2-15.
- [11] A. L. Gurson: In : Fracture 1977, international conference of fracture, Ed. D.M.R. Taplin, 1977, 2A, pp. 357-364.
- [12] A. Needleman, J .R. Rice: In: Mechanics of sheet metal forming, Ed. D.P. Koistinen et al., 1978, Plenum, pp. 237- 267.
- [13] V. Tvergaard: Int. J. Solids and struct. 18 (1982) 659-672.
- [14] V. Tvergaard, A. Needleman: Acta metall. 32 (1984) 157-169.
- [15] A. L. Gurson: J. Eng. Mater. and Technol. 99 (1977) 2-15.
- [16] G. Perrin, J.B. Leblond.: Int. J. Plast. 6 (1990) 677-699.
- [17] I. Wisilius: Fatig. Fract. Eng. Mater. Struct. (2000) 1460-2695
- [18] P. W. Bridgman: Trans. ASM 32 (1944) 553-574.
- [19] Nadai A., 'Theory of flow and fracture of solids', Mc Graw-Hill, New York 1950.